Anthrax pathogen evades the mammalian immune system through stealth siderophore production

Rebecca J. Abergel*, Melissa K. Wilson†, Jean E. L. Arceneaux†, Trisha M. Hoette*, Roland K. Strong‡, B. Rowe Byers†, and Kenneth N. Raymond*§

*Department of Chemistry, University of California, Berkeley, CA 94720-1460; †Department of Microbiology, University of Mississippi Medical Center, Jackson, MS 39216-4505; and ‡Division of Basic Sciences, Fred Hutchinson Cancer Research Center, Seattle, WA 98109

Edited by Harry B. Gray, California Institute of Technology, Pasadena, CA, and approved October 11, 2006 (received for review August 14, 2006)

Systemic anthrax, caused by inhalation or ingestion of *Bacillus anthracis* spores, is characterized by rapid microbial growth stages that require iron. Tightly bound and highly regulated in a mammalian host, iron is scarce during an infection. To scavenge iron from its environment, *B. anthracis* synthesizes by independent pathways two small molecules, the siderophores bacillibactin (BB) and petrobactin (PB). Despite the great efficiency of BB at chelating iron, PB may be the only siderophore necessary to ensure full virulence of the pathogen. In the present work, we show that BB is specifically bound by siderocalin, a recently discovered innate immune protein that is part of an antibacterial iron-depletion defense. In contrast, neither PB nor its ferric complex is bound by siderocalin. Although BB incorporates the common 2,3-dihydroxybenzoyl iron-chelating subunit, PB is novel in that it incorporates the very unusual 3,4-dihydroxybenzoyl chelating subunit. This structural variation results in a large change in the shape of both the iron complex and the free siderophore that precludes siderocalin binding, a stealthy evasion of the immune system. Our results indicate that the blockade of bacterial siderophore-mediated iron acquisition by siderocalin is not restricted to enteric pathogenic organisms and may be a general defense mechanism against several different bacterial species. Significantly, to evade this innate immune response, *B. anthracis* produces PB, which plays a key role in virulence of the organism. This analysis argues for antianthrax strategies targeting siderophore synthesis and uptake.

bacillibactin | *Bacillus anthracis* | petrobactin | siderocalin

Bacillus anthracis, the causative agent of anthrax, is a Gram-positive, spore-forming organism that can infect through intradermal inoculation, ingestion, or inhalation of spores (1, 2). Spores are dormant forms of the bacillus and are extremely resistant to environmental stress (3). In contrast to skin infections, which often remain localized and can be effectively treated, infections from inhalation of *B. anthracis* spores are usually lethal (2). Because a high rate of mortality can result not only from natural infections but also from intentional release, this virulent mammalian pathogen has recently become notorious as a bioweapon. Understanding the virulence mechanisms of *B. anthracis* and identifying potential antiproliferative targets in this microorganism are therefore of great importance.

A number of studies have shown that formation of a poly-D-glutamic acid capsule, which mediates the invasive stage of the infection, and production of the tripartite anthrax toxin, which mediates the toxigenic stage, are essential for full pathogenicity (1). However, the dramatic growth of *B. anthracis* observed during infection, from the engulfment of the endospores by alveolar macrophages to the release of vegetative bacilli from the lymph-node-associated phagocytes and subsequent blood infection, has led Hanna and coworkers (4) to suggest siderophore biosynthesis as an additional requirement for virulence. Production of low-molecular-weight iron chelators, termed siderophores, is a common mechanism used by bacterial pathogens to mediate their mandatory iron acquisition (5, 6). *B. anthracis* relies on two distinct siderophores, bacillibactin (BB) and petrobactin (PB; Fig. 1), to scavenge iron in iron-poor environments and ensure adequate supply during its rapid growth stages (7–9). At least two gene clusters for siderophore biosynthesis are included in the *B. anthracis* genome (4). The five-gene *bacA-CEBF* (*B. anthracis* catechol) cluster encodes the synthesis of the 2,3-catecholate siderophore BB (9) and is 79% similar to the *dhbACEBF* BB operon of *Bacillus subtilis* (10); in addition, two clustered orthologues of the *iuc* family of citrate siderophore biosynthetic genes (11), named *asbAB* (anthrax siderophore biosynthesis), are required for the biosynthesis of the citrate/3,4-catecholate siderophore PB (9). Whereas deletion of *bacCEBF* had little effect on growth in cultured macrophages, *asbA* was found required for growth in low-iron medium, growth in and cytotoxicity to macrophages, and virulence in mice (4). This result implies that production of PB is necessary for the full pathogenicity of *B. anthracis*. PB, first isolated from the marine bacterium *Marinobacter hydrocarbonoclasticus* (12), is an unusual hexadentate citrate- and 3,4-dihydroxybenzoate-containing natural siderophore (13). To our knowledge, a complete hexadentate 3,4-catecholate siderophore has never been observed in a pathogenic bacterium other than *B. anthracis* and the related *Bacillus cereus*. In contrast, BB incorporates the common 2,3-dihydroxybenzoate iron-binding moieties that are linked to a central trilactone scaffold; this molecular structure is remarkably similar to that of the siderophore archetype enterobactin (Ent; Fig. 1; ref. 14). With a ferric complex formation constant on the order of 10^{48}, BB exhibits a phenomenally high and selective affinity for iron (15). So, what essential property of PB is needed to ensure complete virulence of the anthrax pathogen?

Results and Discussion

A parallel can be drawn between the use of dual BB/PB siderophore-mediated iron uptake systems by *B. anthracis* and the well studied Ent/aerobactin pair of siderophores (Fig. 1) produced by some enteric bacteria such as *Escherichia coli* and *Salmonella enterica* (5). The mammalian protein siderocalin (also called lipocalin 2, NGAL, 24p3, and uterocalin) was recently found to complement the general antibacterial iron-depletion defense of the innate immune system by specifically binding to bacterial ferric- and apo-enterobactin, $[Fe^{III}(Ent)]^{3-}$ and Ent, respectively (Fig. 2; see refs. 16 and 17), preventing significant early bacteraemia or compelling the successful pathogens to produce alternate siderophores that are not bound by siderocalin, such as aerobactin and salmo-

Author contributions: R.J.A. and K.N.R. designed research; R.J.A., M.K.W., and J.E.L.A. performed research; R.J.A., R.K.S., and K.N.R. analyzed data; and R.J.A., T.M.H., R.K.S., B.R.B., and K.N.R. wrote the paper.

The authors declare no conflict of interest.

This article is a PNAS direct submission.

Abbreviations: Ent, enterobactin; BB, bacillibactin; PB, petrobactin; DHBA, dihydroxybenzoic acid.

§To whom correspondence should be addressed. E-mail: raymond@socrates.berkeley.edu.

This article contains supporting information (SI) online at www.pnas.org/cgi/content/full/0607055103DCI.

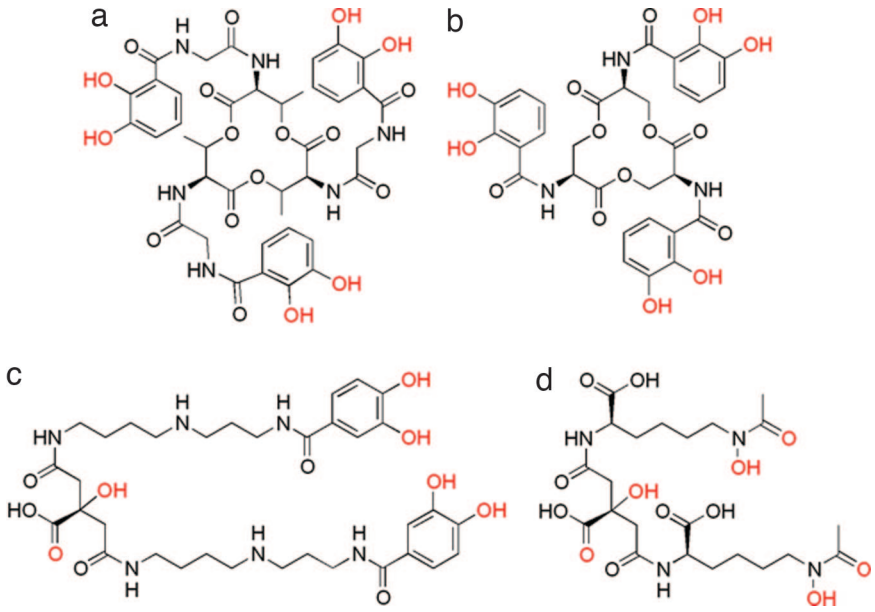

Fig. 1. Molecular structures of *B. anthracis* siderophores (*a* and *b*) and the corresponding siderophores from Gram-negative enteric bacteria (*c* and *d*). (*a*) BB. (*b*) PB. (*c*) Ent.; (*d*) Aerobactin. The iron-coordinating oxygen atoms (when deprotonated) are indicated in red. All completely sequester the Fe^{III} by six-coordinate binding.

chelins (18, 19). In the same manner, *B. anthracis* could resort to the use of PB if BB is a target of the siderocalin immune response; this hypothesis is explored here.

Siderocalin Recognizes BB but Not PB. The affinity of siderocalin for a siderophore can be quantified by monitoring the fluorescence of the protein upon siderophore binding. The equilibrium dissociation constants of siderocalin for BB and its ferric complex were determined at physiological pH (Fig. 3). Analysis of the measured interaction between siderocalin and $[Fe^{III}(BB)]^{3-}$ yielded a K_d value of 0.49 ± 0.02 nM at 20°C. This is an extremely strong affinity, comparable with that observed with $[Fe^{III}(Ent)]^{3-}$, which suggests specific recognition of the ferric siderophore complex (Table 1; ref. 17). The affinity of the protein for the apo form of BB is also indicative of definite binding, as was the case for apo-enterobactin (Table 1; ref. 16). Although some bacterial receptors can discriminate between the two siderophores, such as the *E. coli* native receptor protein FepA, which recognizes only Ent (20), methylation of the trilactone backbone and addition of glycine spacers in BB do not significantly alter recognition by siderocalin of both apo and ferric complex forms. Previous studies have revealed that the siderophore/siderocalin recognition mechanism depends on hybrid electrostatic/cation-π interactions in the highly positively charged protein calyx as well as steric constraints imposed by the conformation of the calyx (17). Hence, neutral ferric complexes of siderophores incorporating hydroxamate and citrate moieties such as aerobactin are not bound by siderocalin, essentially as a result of the lack of electrostatic and cation-π interactions (17).

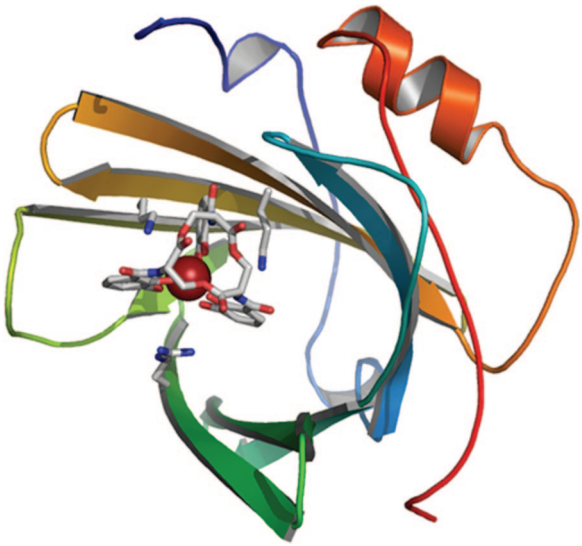

Fig. 2. Crystal structure of the adduct formed by $[Fe^{III}(Ent)]^{3-}$ specifically bound to siderocalin. The specific binding of ferric Ent to siderocalin is caused by hybrid electrostatic/cation-π interactions between $[Fe^{III}(Ent)]^{3-}$ and the side chains of residues Arg-81, Lys-125, and Lys-134 colored by atom type.

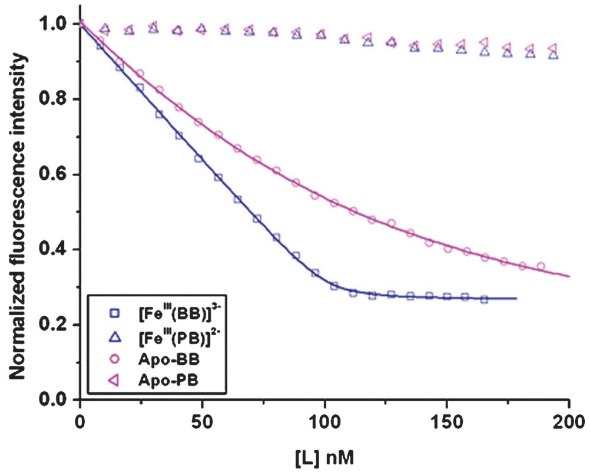

Fig. 3. Fluorescence quenching titrations measuring the affinity of siderocalin for BB, PB, and their ferric complexes. Symbols give the fluorescence measurements at 340 nm (pH 7.4) upon addition of ligand to a 100-nM solution of siderocalin; lines give the calculated fits.

Table 1. Siderocalin affinity for siderophores and their ferric complexes

Siderocalin ligand	K_d, nM (esds)*	Siderocalin ligand	K_d, nM (esds)*
$[Fe^{III}(BB)]^{3-}$	0.49(2)	Apo-BB	31.3(3)
$[Fe^{III}(PB)]^{2-}$	No binding	Apo-PB	No binding
$[Fe^{III}(Ent)]^{3-}$	0.41(11)†	Apo-Ent	3.57(2)†
$[Fe^{III}(TRENglyCAM)]^{3-}$	0.20(2)		
$[Fe^{III}(SERglyCAM)]^{3-}$	0.14(7)		
$[Fe^{III}(_D\text{-Ent})]^{3-}$	0.25(2)		

*Measurements performed at 20°C, in buffered aqueous solutions (pH 7.4).
†The K_d values for enterobactin and its ferric complex were determined in previous studies (16, 17).

Even though the hexadentate ligand PB is similarly built on a citrate bis-spermidine backbone, it contains two 3,4-dihydroxybenzoate iron-binding units linked to the scaffold through amide bonds. The ferric complex of this unusual siderophore $[Fe^{III}(PB)]^{2-}$ is not only negatively charged; it could also participate in cation-π interactions through these catecholamide rings and was therefore a potential candidate for siderocalin binding. However, addition of either the apo form of PB or its ferric complex $[Fe^{III}(PB)]^{2-}$ to siderocalin has no effect on the intensity of the intrinsic fluorescence of the protein (Fig. 3), demonstrating that these compounds do not bind to siderocalin with significant association constants.

Use of 3,4-Catecholate Subunits to Prevent Siderocalin Binding. Although siderocalin has been demonstrated to bind to several diverse siderophores (21), the siderocalin calyx is relatively rigid overall, with only the side chains of two residues, Trp-79 and Arg-81, showing any conformational variation in response to ligand binding, significantly restricting the range of siderophore substituent variation tolerated (17, 21). As shown in Fig. 4, the altered position of the carboxylates of 3,4-catecholate-based siderophores relative to 2,3-catecholate-based siderophores generates major steric clashes with side- and main-chain atoms of several residues in at least two pockets of the calyx (one is defined by the Lys-125 and -134 residues, the other by Lys-134 and Arg-81). This prediction is confirmed by cocrystallization-binding assays of siderocalin in the presence of the tris-bidentate ferric complexes of either 3,4-dihydroxybenzoic acid (DHBA), $[Fe^{III}(3,4\text{-DHBA})_3]^{3-}$ or 2,3-DHBA, $[Fe^{III}(2,3\text{-DHBA})_3]^{3-}$. Colorless protein crystals were obtained in the presence of $[Fe^{III}(3,4\text{-DHBA})_3]^{3-}$, indicative of the absence of the ferric–catecholate complex in the calyx of the protein, because such ferric complexes exhibit a characteristic color resulting from the intense ligand-to-metal charge transfer transitions, yielding strongly colored protein complex crystals when cocrystallized with compounds that do bind, such as $[Fe^{III}(2,3\text{-DHBA})_3]^{3-}$ (16, 17). Thus, the 3,4-catecholate PB is not a substrate of siderocalin and seems likely produced by the pathogen as a stealth siderophore to evade siderocalin inactivation of iron uptake.

Scaffold and Chirality Modifications Do Not Impair Siderocalin Recognition. The nature of the recognition process is necessary to explain the bacteriostatic role of the protein in siderophore interception. Consequently, the specificity of siderocalin for hexadentate tripodal 2,3-catecholamide ligands was probed by using TRENglyCAM, SERglyCAM, and enantio-enterobactin ($_D$-Ent), all analogues of BB and Ent built on different synthetically accessible backbones (Fig. 5; refs. 22 and 23). Fluorescence-binding titrations were performed on their ferric complexes [supporting information (SI) Figs. 6–8], which were all

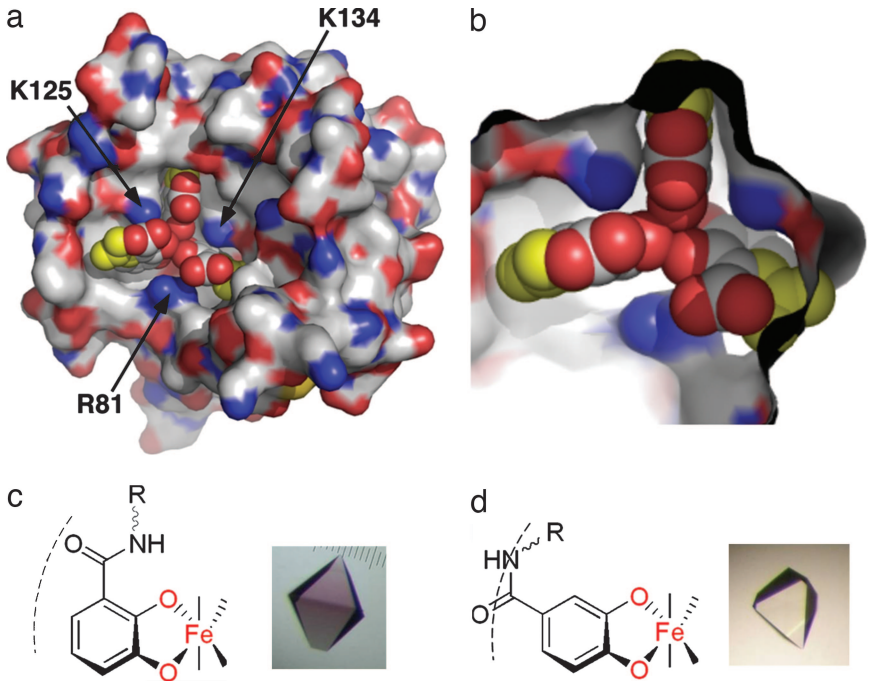

Fig. 4. Comparison of the tris-bidentate complexes $[Fe^{III}(2,3\text{-DHBA})_3]^{3-}$ and $[Fe^{III}(3,4\text{-DHBA})_3]^{3-}$ for siderocalin binding. (*a*) A view of the crystal structure of the tris-bidentate ferric complex of 2,3-DHBA, $[Fe^{III}(2,3\text{-DHBA})_3]^{3-}$ bound to siderocalin. Steric conflicts between siderocalin and the carboxyl groups of a 3,4-DHBA complex (yellow) are generated in simulated binding. (*b*) A cutaway showing the penetration of the protein surface by $[Fe^{III}(3,4\text{-DHBA})_3]^{3-}$ in two of the pockets during simulated binding. (*c*) Molecular structure of a 2,3-dihydroxybenzoyl subunit bound to iron. The dashed arc represents the wall of the protein calyx. Cocrystallization of siderocalin with $[Fe^{III}(2,3\text{-DHBA})_3]^{3-}$ gives red crystals, indicative of binding. (*d*) Molecular structure of a 3,4-dihydroxybenzoyl subunit bound to iron. The dashed arc represents the wall of the protein calyx. Cocrystallization of siderocalin with $[Fe^{III}(3,4\text{-DHBA})_3]^{3-}$ gives colorless crystals, suggestive of nonbinding.

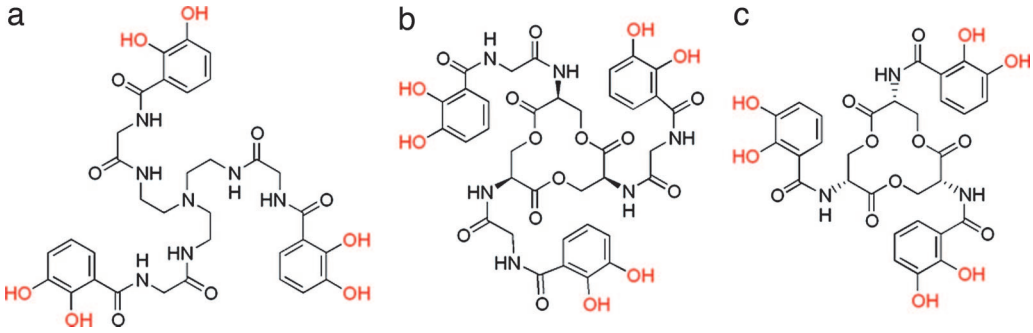

Fig. 5. Synthetic analogues of BB and Ent. (*a*) TRENglyCAM. (*b*) SERglyCAM. (*c*) $_{D}$-Ent. The iron-coordinating oxygen atoms (when deprotonated) are in red.

found to bind siderocalin very tightly, with K_d values on the same order of magnitude as $[Fe^{III}(BB)]^{3-}$ and $[Fe^{III}(Ent)]^{3-}$ (Table 1). The similar equilibrium dissociation constants obtained for these ferric complexes confirm that neither replacement of the trithreonine backbone by the triserine or the tripodal tris(2-aminoethyl)amine scaffolds (16) nor the presence of the glycine spacers affects siderocalin binding. Moreover, the trilactone-based siderophore complexes $[Fe^{III}(Ent)]^{3-}$ (Δ), $[Fe^{III}(_{D}\text{-Ent})]^{3-}$ (Λ), $[Fe^{III}(BB)]^{3-}$ (Λ), and $[Fe^{III}(SERglyCAM)]^{3-}$ (Λ) constitute a series of complexes with different metal center chiralities (22, 23). Hence, metal center chirality is not a distinguishing feature for siderocalin.

PB Is Used for Both Microbial Iron Transport and Immunoevasion. Although a number of different natural and synthetic siderophore ferric complexes bind to siderocalin, protein recognition remains very specific to ligands incorporating small cation-π systems such as unsubstituted 2,3-catecholamide rings. The 2,3-dihydroxybenzoate iron-chelating moiety is very common among siderophores used by pathogens (5). Although these siderophores exhibit the highest affinities for ferric ion (14, 15) and the fastest rates at removing iron from host proteins such as transferrin (24), they are usually produced together with complementary iron scavengers incorporating hydroxamate or citrate-binding units (5). Some pathogenic strains of Gram-negative bacteria, including *Salmonella typhimurium* LT2 and *E. coli* CFT073, also harbor the five-gene *iroA* locus that enables the production of bulky C-glycosylated Ent analogues, salmochelins (25). Recent studies have confirmed that production of these additional siderophores is a bacterial strategy to evade the specific siderocalin-associated mechanism of the innate immune system (16, 18). The BB/PB pair is another example of such bacterial evasion that we suspect may be a universal phenomenon; for instance, the plant pathogenic enterobacterium *Erwinia chrysanthemi* produces the 2,3-catecholate siderophore chrysobactin, but its full virulence requires synthesis of the citrate siderophore achromobactin (26). However, the use of the 3,4-catecholate PB by *B. anthracis* and *B. cereus* remains notable (9, 27). Few studies have analyzed the thermodynamics of iron binding through 3,4-catecholamide fragments (28); although such chelating units exhibit a slightly lower affinity for Fe^{3+} and greater sensitivity to oxidation than that observed with 2,3-catecholamides, they are significantly more efficient at binding ferric ion than hydroxamates or citrates. Moreover, *B. anthracis* uses transferrin-bound iron as a sole source of the metal (7), and *B. cereus* was shown to use this iron source during infection (29). The 2,3-catecholamides iron-chelating subunits are known for their advantageous high kinetic rates of iron removal from diferric-transferrin as compared with hydroxamates (24). Because a number of differently functionalized simple catecholate ligands are known to catalyze this iron removal, it seems likely that this will also be so for 3,4-catecholamide siderophores (30).

Conclusion

This study shows that dual production of the siderophores BB/PB by *B. anthracis* is not redundant. The mammalian protein siderocalin binds specifically to both the apo form of BB and its ferric complex, as well as to various analogues of BB and Ent, whereas PB, which incorporates 3,4-catecholamide as a chelating group, is not a substrate for sequestration by siderocalin. Thus, virulence of the zoonotic agent *B. anthracis* and the opportunistic human pathogen *B. cereus* is ensured through production of an unparalleled siderophore, likely as a response to siderocalin-mediated iron depletion. Because PB is not known to be produced by any other *Bacillus* species, antianthrax strategies that target PB synthesis and uptake may be effective therapeutics while sparing commensal bacteria.

Materials and Methods

Siderophore Production. BB and PB were isolated from low-iron culture filtrates of *B. cereus* ATCC 14579 and *B. anthracis* USAMRIID, respectively, and purified as reported (9). The ligands TRENglyCAM (23), SERglyCAM (22), and $_{D}$-Ent (23) were prepared according to described procedures.

Protein-Binding Assay. Recombinant siderocalin was prepared as described (17) and stored at millimolar concentrations in PBS aqueous buffer (pH 7.4) at 4°C. Fluorescence quenching of recombinant siderocalin was measured on a Jobin Yvon (Longjumeau, France) fluoroLOG-3 fluorometer with 3-nm-slit band pass, using the characteristic excitation and emission wavelengths λ_{exc} = 281 nm and λ_{em} = 340 nm. Measurements were made at a protein concentration of 100 nM in Tris-buffered saline (pH 7.4)/5% DMSO/32 μg/ml ubiquitin (Sigma, St. Louis, MO). Fluorescence values were corrected for dilution upon addition of ligand (5-min equilibration time after each aliquot addition), and data were analyzed by nonlinear regression analysis of fluorescence response vs. ligand concentration using a one-site binding model as implemented in DYNAFIT (31). The substrate solutions were freshly prepared *in situ*. An aliquot of a DMSO stock solution of the free ligand (4 mM, 25 μl) and $FeCl_3$ (27 mM, 1 equiv) were combined, vigorously shaken, and diluted with TBS buffer to form the ferric complexes at a concentration of 0.1 mM (no metal added in the case of apo-siderophores). The solutions were equilibrated for 2 h and diluted to a final concentration of 6 μM in 5% DMSO/TBS aqueous buffer (pH 7.4). Recombinant siderocalin was cocrystallized with test $[Fe^{III}(2,3\text{-DHBA})_3]^{3-}$ and $[Fe^{III}(3,4\text{-DHBA})_3]^{3-}$ as described (17).

This work was supported by National Institutes of Health Grants AI11744 (to K.N.R.) and AI59432 (to R.K.S.) and by the Intramural Research Support Grant Program at the University of Mississippi Medical Center (to B.R.B.).

1. Dixon TC, Meselson M, Guillemin J, Hanna PC (1999) *N Engl J Med* 341:815–826.
2. Friedlander AM (2000) *Curr Clin Top Infect Dis* 20:335–349.
3. Spencer RC (2003) *J Clin Pathol* 56:182–187.
4. Cendrowski S, MacArthur W, Hanna PC (2004) *Mol Microbiol* 51:407–417.
5. Dertz EA, Raymond KN (2003) in *Comprehensive Coordination Chemistry II*, eds McCleverty J, Meyer T (Pergamon, Oxford), Vol 8, pp 141–168.
6. Goswami T, Rolfs A, Hediger MA (2002) *Biochem Cell Biol* 80:679–689.
7. Garner BL, Arceneaux JEL, Byers BR (2004) *Curr Microbiol* 49:89–94.
8. Koppisch AT, Browder CC, Moe AM, Shelley JT, Kinkel BA, Hersman LE, Iyer S, Ruggiero CE (2005) *Bio Metals* 18:577–585.
9. Wilson MK, Abergel RJ, Raymond KN, Arceneaux JEL, Byers BR (2006) *Biochem Biophys Res Comm* 348:320–325.
10. May JJ, Wendrich TM, Marahiel MA (2001) *J Biol Chem* 276:7209–7217.
11. Challis G (2005) *Chem Biochem* 6:601–611.
12. Barbeau K, Zhang GP, Live DH, Butler A (2002) *J Am Chem Soc* 124:378–379.
13. Bergeron RJ, Huang GF, Smith RE, Bharti N, McManis JS, Butler A (2003) *Tetrahedron* 59:2007–2014.
14. Raymond KN, Dertz EA, Kim SS (2003) *Proc Natl Acad Sci USA* 100:3584–3588.
15. Dertz EA, Xu J, Stintzi A, Raymond KN (2006) *J Am Chem Soc* 128:22–23.
16. Abergel RJ, Moore EG, Strong RK, Raymond KN (2006) *J Am Chem Soc* 128:10998–10999.
17. Goetz DH, Holmes MA, Borregaard N, Bluhm ME, Raymond KN, Strong RK (2002) *Mol Cell* 10:1033–1043.
18. Fischbach MA, Lin H, Zhou L, Yu Y, Abergel RJ, Liu DR, Raymond KN, Wanner BL, Strong RK, Walsh CT, *et al.* (2006), *Proc Natl Acad Sci USA* 103:16502–16507.
19. Flo TH, Smith KD, Sato S, Rodriguez DJ, Holmes MA, Strong RK, Akira S, Aderem A (2004) *Nature* 432:917–921.
20. Annamalai R, Jin B, Cao Z, Newton SMC, Klebba PE (2004) *J Bacteriol* 186:3578–3589.
21. Holmes MA, Paulsene W, Jide X, Ratledge C, Strong RK (2005) *Structure (London)* 13:29–41.
22. Bluhm ME, Kim SS, Dertz EA, Raymond KN (2002) *J Am Chem Soc* 124:2436–2437.
23. Dertz EA, Xu J, Raymond KN (2006) *Inorg Chem* 45:5465–5478.
24. Turcot I, Stintzi A, Xu JD, Raymond KN (2000) *J Biol Inorg Chem* 5:634–641.
25. Fischbach MA, Lin H, Liu DR, Walsh CT (2006) *Nat Chem Biol* 2:132–138.
26. Franza T, Mahe B, Expert D (2005) *Mol Microbiol* 55:261–275.
27. Harvie DR, Ellar DJ (2005) *Curr Microbiol* 50:246–250.
28. El Hage Chahine JM, Bauer AM, Baraldo K, Lion C, Ramiandraosa F, Kunesch G (2001) *Eur J Inorg Chem* 2001:2287–2296.
29. Park RY, Choi MH, Sun HY, Shin SH (2005) *Biol Pharm Bull* 28:1132–1135.
30. Nguyen SAK, Craig A, Raymond KN (1993) *J Am Chem Soc* 115:6758–6764.
31. Kuzmic P (1996) *Anal Biochem* 237:260–273.